Combined Rheological and Ultrasonic Study of Alginate and Pectin Gels near the Sol−Gel Transition

Michel Audebrand,[†] Max Kolb,[‡] and Monique A. V. Axelos*,[†]

Biopolymères, Interactions, Assemblages UR 1268, Institut National de la Recherche Agronomique, B.P. 71627, Rue de la Géraudière, 44316 Nantes CEDEX 03, France, and Laboratoire de Chimie, Ecole Normale Supérieure, 46 allée d'Italie, 69364 Lyon CEDEX 07, France

Received March 27, 2006; Revised Manuscript Received July 3, 2006

The sol−gel transition of biopolymer mixtures has been investigated by rheological and ultrasonic measurements. A scaling analysis of the data was performed for both types of measurements. A gel time was determined from rheology for the pure pectin samples, and the data could be fitted to a universal scaling form near the transition point. Its critical exponents are in good agreement with the predictions of scalar percolation theory. In addition, the ultrasonic signal of the pectin samples close to the transition was analyzed in terms of a high-frequency scaling approach for the attenuation and the velocity. For the alginate samples and the mixtures, for which the gel point cannot be determined reliably from rheology, the ultrasonic measurements were analyzed using the same scaling form as for the pectin sample, thus providing a method for estimating the gel point, even in the absence of rheological data.

1. Introduction

It is by now well-understood that the gelation transition in polymer systems is the result of random bond formation between monomers in a liquid phase (sol), which eventually leads to a highly elastic, cross-linked network (gel). The dynamic properties of gelling systems have been extensively studied in the past. Rheological measurements on either chemical or physical gels during the gelation process have shown power-law behavior for many physically relevant quantities.[1−4] This phenomenon is a generic feature of a gelation transition and is observed for diverse gelling systems such as biopolymers (pectin, alginate), cross-linked polyurethane,[5] and chromium-induced gelation of polyacrylamide.[6] The classical theory of the gelation transition was originally developed by Flory[7] and by Stockmayer.[8] A detailed description of critical phenomena near the gel point was given much later in terms of percolation theory.[9] This theory quantitatively describes the connectivity properties that result from random bond formation on a D-dimensional lattice and predicts universal scaling behavior for structural and dynamical properties. If p denotes the fraction of bonds formed, the sol-to-gel transition occurs at p_c (the percolation threshold) when the linear size of the largest cluster ξ (the correlation length) becomes infinite. ξ is expected to scale as $\xi \sim \epsilon^{-\nu}$ in terms of the dimensionless measure $\epsilon = |p - p_c|/p_c$. For an experimental system, p is the density of cross-links and p_c its value at the gel point. The critical exponent ν is universal in the sense that it does not depend on material details.

The rheological properties of a viscoelastic system can be characterized by the complex shear modulus $G^* = G' + iG''$ or the related complex viscosity $\eta^* = G^*/i\omega$. These viscoelastic quantities are also expected to behave in a singular way near p_c, and the corresponding scaling laws define the dynamical critical exponents s, t, and Δ: $\eta_0 \sim \epsilon^{-s}$ below the transition, $G_0 \sim \epsilon^t$ above the transition, and $G' \sim G'' \sim \omega^\Delta$ at the transition. Here, η_0 is the static (zero frequency) viscosity, G_0 the static elastic modulus, and G' and G'' are the storage and loss part of the complex shear modulus as a function of frequency ω.

These scaling laws are specific predictions of a general scaling form for the complex shear modulus $G^*(\omega, \epsilon)$, originally proposed by Efros and Shklovskii[10] for the electrical analogue of G^* and valid in the limit of $\omega, \epsilon \rightarrow 0$

$$G^*(\omega, \epsilon) = G_0(\epsilon)\, \phi(i\omega/\omega_0) \tag{1}$$

where $\omega_0 \sim \epsilon^{s+t}$ is the characteristic frequency (the inverse of the longest relaxation time) and ϕ a universal scaling function. At low frequency, outside the critical region ($\omega \ll \omega_0$) where the system is homogeneous, G^* behaves as $G' \sim \omega^2$, $G'' \sim \omega$ below the gel point and $G' \sim$ constant, $G'' \sim \omega$ above the gel point. Inside the critical region ($\omega \gg \omega_0$), both below and above the transition, $G' \sim G'' \sim \omega^\Delta$ with $\Delta = t/(s + t)$ and $G''/G' = \tan(\Delta\pi/2)$.[11] On the basis of this scaling description, a robust, widely used criterion to identify the gel point and the exponent Δ associated with the transition has been proposed by Winter and Chambon.[12,13] One plots, for different frequencies ω, the ratio G''/G' as a function of time and considers the (unique) crossing point of the different curves to be the gel point. Furthermore, the value of G''/G' at the gel point directly determines the exponent Δ.

During the past decade, it has been shown that information on the properties of materials can be obtained from ultrasonic measurements, used as a high-frequency structural probe.[14] In particular, the method has been used to monitor the structural changes of gelling systems, for both chemical[15,16] and physical gel.[17,18]

The physics of an ultrasonic probe are very different from the physics of a rheological measurement. The theory of a longitudinal ultrasonic wave traveling in a viscoelastic material has been established for a long time.[14] The velocity v and the attenuation α of a longitudinal wave can be related to the complex longitudinal modulus $M^* = M' + iM''$ as follows:

$$M' = K' + \frac{4}{3} G' = \rho v^2 \tag{2a}$$

$$M'' = K'' + \frac{4}{3} G'' = \frac{2\rho\alpha\, v^3}{\omega} \Rightarrow \frac{M''}{\omega} = \frac{2\rho\alpha v^3}{\omega^2} = \zeta + \frac{4}{3}\eta \tag{2b}$$

[†] Institut National de la Recherche Agronomique.
[‡] Ecole Normale Supérieure.

10.1021/bm060297e CCC: $33.50
Published on Web 09/21/2006

where ρ is the density, K' and K'' are, respectively, the real and imaginary part of the bulk modulus, G' and G'' the real and imaginary part of the shear modulus, $\omega = 2\pi f$ the angular frequency, ζ the bulk viscosity, and η the shear viscosity.

A main issue is whether ultrasounds do exhibit singular behavior at the transition point. More specifically, do the velocity and the attenuation coefficient behave singularly at the onset of the network formation, and are ultrasonic measurements related to rheological measurements? In earlier work,[17] it has been shown that in weak gels (~99% water) ultrasonic measurements are very sensitive to the state of aggregation of the gelation process, but it is impossible to separate the bulk and shear contributions of the measured moduli. In such gels, the network formation involves only electrostatic interactions without a change in density. Therefore, even though the contribution from the bulk modulus is dominant, gelation can still be monitored by ultrasounds as long as one assumes that the bulk modulus remains constant, and only the shear modulus changes with the evolution of the gelation process. This assumption may be justified by the fact that at low polymer concentration the cross-link density is very low, and its change during gelation is even lower.

To our knowledge, up to now there has been only one study that attempts a quantitative scaling analysis of ultrasonic measurements during gelation.[15] In this investigation, Sidebottom interprets the critical behavior of an epoxy resin near its sol−gel transition in terms of a scaling theory that differs significantly from the low-frequency scaling theory of Efros and Shkolovskii.[10] The critical exponents derived from this high-frequency model are not the same as the exponents for the rheological properties at low frequency, but the following set of relations have been derived.[15]

In the low-frequency limit (rheology)

$$\eta_0 \sim \epsilon^{-k_\infty} \qquad k_0 = t_\infty(1/u - 1) \qquad p < p_c \tag{3a}$$

$$G_0 \sim \epsilon^{t_\infty} \qquad t_0 = t_\infty(1/u + 1) \qquad p > p_c \tag{3b}$$

and in the high-frequency limit (ultrasounds)

$$\eta \sim \epsilon^{-k_\infty} \qquad k_\infty = t_\infty(2/u - 1) \qquad p < p_c \tag{3c}$$

$$G' \sim \epsilon^{t_\infty} \qquad p > p_c \tag{3d}$$

and near p_c

$$G' \sim \omega^u \tag{3e}$$

In his study of epoxy resins close to the sol−gel transition[15] (a strong gel as opposed to the weak gels considered here), Sidebottom applies these expressions and assumed furthermore that relaxation phenomena are absent in the frequency range considered. Equations 2 can then be written as

$$\Delta v^2 \sim G' \sim \epsilon^{t_\infty} \tag{4a}$$

$$\Delta(\alpha v^3) \sim \eta \sim \epsilon^{-k_\infty} \tag{4b}$$

The Δ in eq 4 signifies that relative values must be used. In practice, we have subtracted from the velocity and the attenuation their value at the beginning of the experiment. For the epoxy resins,[15] the values for t_∞ and k_∞ obtained from these equations are $t_\infty = 0.47$ and $k_\infty = 4$, respectively.

Several others experimental investigations have tried to find an ultrasonic signature of the sol−gel transition. Ratajaska et al.[19] attempted to extract critical exponents from a combined measurement of fluorescence intensity and ultrasound velocity for two gelling materials, silica (TMOS) and aqueous gelatin, and interprets them in terms of the percolation theory. The dynamical features of the two gels differ, but the measured (universal) exponents agree to within experimental errors. In Lairez et al.,[20] gelation of epoxy was monitored by rheology and by ultrasound. The peak of the relative attenuation and the inflection point of the relative velocity occur prior to the gel point as determined by rheology, but the result might be influenced by the proximity of the glass transition. In an earlier study by Bacri et al.,[18] the attenuation is used to determine T_g, the gel fraction, and the associated exponent β for polyacrylamide and gelatin.

We conclude that there is no generally valid criterion for identifying the transition point from ultrasonic measurements. This contrasts with rheology, where percolation theory provides a microscopic basis for static and dynamic properties near the transition. To better understand the ultrasonic data, we have undertaken a combined rheological and ultrasonic study. We have chosen to investigate calcium-induced pectin and alginate model gels, because they are well-characterized[21,22] and because they fully confirm the theoretical prediction for the rheological behavior near the transition.[3,4]

2. Materials and Methods

2.1. Pectin. Pectin consists of randomly connected α-(1,4)-D-galacturonic acid units and their methyl esters. The citrus pectin used in this study was a sample supplied by Copenhagen Pectin (Denmark) and is referenced as Genu pectin type X-6010. The fraction of galacturonic residues which were esterified was 47%, and its intrinsic viscosity measured at 20 °C in 0.1 M Nacl was $[\eta] = 0.336$ L/g.

2.2. Alginate. Alginates are binary heteropolymers consisting of α-L-guluronic acid (G) and β-D-mannuronic acid (M) in various proportion and sequences. The two different monomers are distributed in a block pattern with pure M-blocks and pure G-blocks. Each polymer then consists of a sequence of blocks of varying length. We have used a sodium alginate sample isolated from *Laminaria hyperborea* stipe kindly provided by Kurt Draget from NOBIPOL in Trondheim, Norway. Its guluronic content was 68%, and its intrinsic viscosity at 20 °C in 0.1 M NaCl was $[\eta] = 0.520$ L/g. The dependence of the gel properties on the alginate parameters has been described in ref 23.

2.3. Preparation of Gels. Both polymers are able to form a gel in the presence of divalent cations such as calcium. In pectin gels, junction zones result from the lateral association of homogalacturonic acid chain sequences induced by the chelation of the calcium ions.[24] In alginate gels, only the G-block sequences can be associated by calcium into dimers or multimers.[25]

Following the recipe already published by the NOBIPOL group,[25] the polymer powder was dispersed in deionized water under high-speed magnetic stirring in order to obtain a ~2% (w/w) solution. After adjusting the pH to 7, these stock solutions were filtered and stored at 4 °C. The calcium ions were added in two different ways. In the first one, a solution of CaEGTA was added, and in the second one, calcium carbonate powder was added directly. In both cases, a progressive release of calcium ions was induced by slowly decreasing the pH through the addition of glucono-δ-lactone (GDL). The gelation rate depends on the amount of calcium ions freed.

2.3.1. Gelling by CaEGTA. A 100 mM stock solution of CaEGTA was prepared by dispersing 3.8 g EGTA in 50 mL of deionized water together with 1.47 g $CaCl_2 \cdot 2H_2O$. The pH was adjusted to 7 by adding approximately 30 to 40 mL of 1 M NaOH, and then, the volume was adjusted to 100 mL by adding water. For a maximum release of Ca^{2+} from CaEGTA, the stoichiometric ratio [GDL]/[CaEGTA] must be close to 4. The GDL solution (in water) must be prepared just before being

Table 1. Composition of the Samples Used in This Study

polymer	calcium	GDL	sample
pectin 1%	30 mM CaEGTA	120 mM	Pe 1 30 120
pectin 1%	15 mM $CaCO_3$	30 mM	Pe 1 15 30
alginate 1%	15 mM $CaCO_3$	30 mM	Al 1 15 30
alginate 0.25% + pectin 0.75%	15 mM $CaCO_3$	30 mM	25/75
alginate 0.5% + pectin 0.5%	15 mM $CaCO_3$	30 mM	50/50
alginate 0.75% + pectin 0.25%	15 mM $CaCO_3$	30 mM	75/25

added. Its concentration was calculated from the desired final composition of the mixture. Appropriate amounts of each solution (polymer, CaEGTA, GDL) were mixed together in order to obtain a final polymer concentration of 1%. The amounts of CaEGTA and GDL were chosen according to the desired gelation rate. We have worked with 30 mM of CaEGTA. Under these conditions, the final pH was ~4.7.

2.3.2. Gelling by $CaCO_3$. The $CaCO_3$ powder must have a very small average particle size to prevent sedimentation and the formation of an inhomogeneous gel. We have used an "Eskal 500" quality powder with average particle size below 10 μm. An appropriate amount of $CaCO_3$ powder was first dispersed in 1 or 2 mL of water. Polymer and GDL solutions were then added. To ensure a complete freeing of all Ca^{2+} and a final pH in the gel of ~6, the molar concentration of GDL must be compared twice with $CaCO_3$. In most cases, we have worked with 15 mM $CaCO_3$. Time was measured from the moment when GDL was added (under stirring). To avoid sound scattering by CO_2 or air bubbles, the mixture was degassed at low pressure before being poured into the measurement cell. Table 1 summarizes the compositions of the different samples used.

2.4. Rheology. Small-amplitude oscillatory shear experiments were performed at 25 °C using a Rheometrics fluid spectrometer (RFSII) with cone-plate geometry (5 cm diameter; 1° cone angle). This apparatus was programmed to record a series of mechanical spectra during gel formation. The frequency range of the spectra was chosen to cover a fairly large range (0.6−60 rad/s) and still execute rapidly enough. Under these conditions, the apparatus takes 2 min to record an entire spectrum. Measurements were carried with a strain amplitude of 5%.

2.5. Ultrasounds. The change in ultrasonic velocity and attenuation coefficient of the samples were measured using the same experimental setup as described in detail by Audebrand.[17] The sample was placed in a cylindrical measurement cell which was kept at 25 °C by a thermostated bath. Two commercial transducers with nominal frequency of 50 MHz were tightly fitted on each side of the cell; the path length is defined by moving them along their axes. The path length was taken as ~1 cm (i.e., a cell volume of ~2 mL). The first transducer was excited with a pulse, and the transmitted longitudinal wave was then processed with a fast Fourier transform analysis (FFT). By taking the first sample as reference, the comparison of the amplitude spectrum of the FFT during the gelation process allowed us to determine the frequency dependence of the relative absorption $\Delta\alpha(\omega)$. In the same way, from the comparison of the phase spectrum the frequency dependence of the relative velocity $\Delta v(\omega)$ was obtained. The change in ultrasonic velocity and attenuation was measured at 25 MHz, which corresponds to the peak of the attenuation spectrum. Experimental data were acquired automatically at 4 min intervals.

3. Results and Discussion

3.1. Pectin Gelation. We have considered pectin gelation by the two different Ca release mechanisms in order to investigate the influence of the reaction speed and the homogeneity of the release mechanism. Both samples yield comparable rheological and ultrasonic transition properties, with the slower and more homogeneous mechanism producing better scaling results over a wider range in frequency.

3.1.1. Gelling by CaEGTA. Figure 1 is an example of the mechanical spectra obtained during the gelation of a 1% (w/w) pectin solution with 30 mM CaEGTA and 120 mM GDL

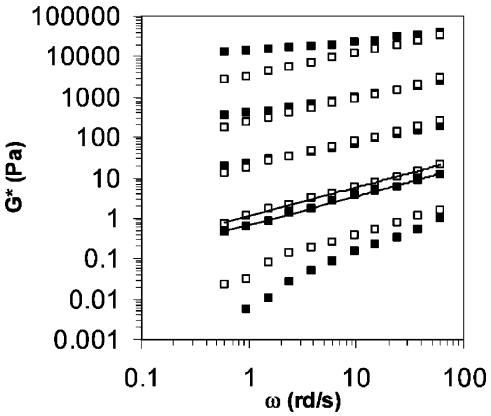

Figure 1. Frequency dependence of the moduli G' (■) and G'' (□) at several stages of the gelation process of pectin Pe 1 30 120. The bottom spectrum, at $t = 2520$ s, is below the gel point; the next one, at $t = 3030$ s, is at the gel point; and the following three, at $t = 3532$, 3782, and 4533 s, are above the transition. For better visualization, each spectrum has been shifted upward vertically by one decade with respect to the previous one.

(sample Pe 1 30 120). Five data series for G' (solid) and G'' (open) below, at and above the transition are shown. For easier visualization, each series is shifted vertically by one decade with respect to the previous one. The first spectrum was taken at the beginning of the gelation process. G' and G'' behave as in a macromolecular solution; their low-frequency behavior approaches the expected limiting power law, with slopes of 2 for G' and 1 for G''. Measurements at even lower frequencies, below and at the transition, are limited by the sensitivity of the device. With time, due to the steady release of calcium ions (induced by GDL hydrolysis upon lowering of the pH), small isolated clusters grow in solution, and the moduli begin to increase gradually. Progressively, new clusters form, and existing clusters aggregate up until they form a percolating network at the gel point (T_g). The next spectrum in the series was recorded at T_g, to within 1 min. As predicted by theory, both G' and G'' exhibit a power-law behavior with a universal exponent $\Delta = 0.7$ which extends over the entire frequency range ($G' \sim G'' \sim \omega^{0.7}$). This agrees with the exponent already found for other weak gels.[3,4] At T_g, the total amount of calcium has not yet been released. The pH continues to decrease, and further release of Ca^{2+} creates additional cross-links which increases the strength of the gel. This can be seen on the later spectra, above the gel point, where G' necessarily crosses G'' as the former becomes constant at low frequency. Three such spectra are shown at the top of the figure. All are characteristic of a gel. The data qualitatively confirms the behavior predicted by theory. At low frequency, the material behaves like an elastic medium with a storage modulus G' which is frequency-independent and a loss modulus G'' which decreases with decreasing ω. With increasing time or extent of reaction, the crossing frequency ω_x and the corresponding crossing point modulus $G_x \equiv G'_x = G''_x$ increase and satisfy $G_x \sim \omega_x^{\Delta}$.

Another method to determine the gel point is to identify the time when the zero-frequency viscosity diverges or the static elastic modulus vanishes. In Figure 2, the gel point T_g and the critical exponents k_0 and t_0 are estimated from the mechanical spectra $\eta_0(t)$ and $G_0(t)$ close to the transition. η_0 and G_0 are obtained from extrapolating the finite frequency measurements to zero frequency. Below the gel point, the viscosity was plotted in the form η_0^{-1/k_0} as a function of time, with k_0 a critical exponent. By adjusting k_0 to have the best straight line behavior close to the gel point, we obtain $T_g = 3058(20)$ s and $k_0 = 0.70(2)$. In practice, the points very close to the gel point are

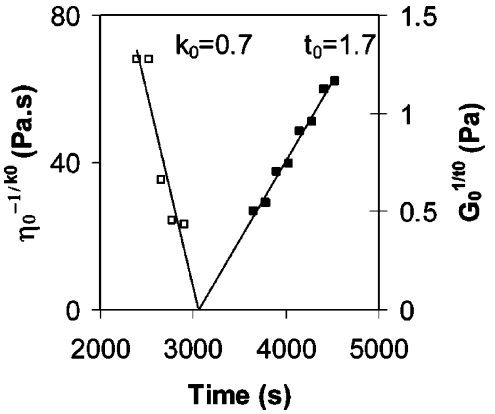

Figure 2. Scaling analysis for the rheological data of the Pe 1 30 120 sample. The zero frequency viscosity (□) and elastic modulus (■) are plotted in scaling form, $\eta_0^{-1/k_0} \propto (T_g - T)$ and $G_0^{1/t_0} \propto (T - T_g)$, respectively. The exponents k_0 and t_0 are varied to obtain the best straight line near the transition. Both data sets extrapolate to the same gel time, $T_g = 3058$ s.

not taken into account, because the finite frequency measurements cannot be extrapolated reliably to zero frequency. Similarly, data points too far from the gel point deviate from the scaling fit as they lie outside the scaling range. The value for T_g obtained from η_0 coincides with the one obtained from the mechanical spectra in Figure 1. From adjusting G_0^{1/t_0} above the gel point in the same way, we find $t_0 = 1.70(2)$ and the same gel point. The estimates for T_g from η_0 and G_0 are consistent with each other. A more stringent combined fit of η_0 and G_0—imposing a common gel point—also yields the same estimates for T_g and the exponents. Both exponents are in good agreement with previous experiments[3] and with theory.[1] In addition, they satisfy the exponent relation predicted by scaling theory: $\Delta = t_0/(k_0 + t_0)$. In general, for the weak gels under consideration here, collecting data below the gel point is difficult because of the fluctuations due to the limited sensitivity of the rheometer and also because the measurement times at low frequency become too long such that the system may evolve during a measurement.

We have also tried the Winter−Chambon method[12,13] of identifying the gel point. Because of strong fluctuations of G' below and near the gel point, the curves do not cross in a unique point.

The scaling aspect can be emphasized by plotting the data differently and considering the ratio $G''(\omega, \epsilon)/G'(\omega, \epsilon) = \phi''(i\omega/\omega_0)/\phi'(i\omega/\omega_0)$ as a function of ω. As can be seen from eq 1, this has the advantage that the term $G_0(\epsilon)$ is eliminated from the scaling expression, and the resulting scaling function only depends on the single variable ω/ω_0. At high frequency ($\omega \gg \omega_0$), one expects the ratio G''/G' to be constant; at low frequency ($\omega \ll \omega_0$), it rises (linearly) below T_g and decreases (linearly) above T_g. Furthermore, the constant value of G''/G' at high frequency is equal to $\tan(\Delta\pi/2)$. The changing of the slope at low frequency identifies the gel time T_g. All these features are verified for the Pe 1 30 120 sample, as shown in Figure 3. From the figure, we also conclude that the crossover region between the low-frequency regimes and the high-frequency regime is rather broad.

In parallel with the rheological measurements, the ultrasonic data have been recorded for all the samples studied. Figure 4 shows the evolution with time of the relative attenuation $\Delta\alpha$ and the relative velocity Δv at 25 MHz for Pe 1 30 120. The first data point always serves as a reference for the relative measurements used in the analysis. During the first 15 000 s,

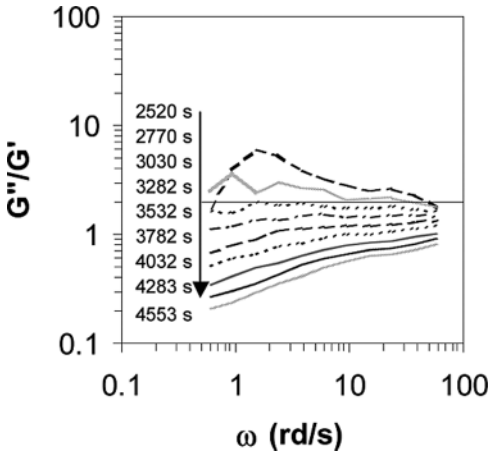

Figure 3. Ratio G''/G' as a function of ω for Pe 1 30 120 at different times (log−log). From top to bottom, the curves correspond to increasing measurement times across the gel point. The horizontal line corresponds to the transition point $G''/G' = \tan(\Delta\pi/2)$, with $\Delta = 0.71$. At high frequency, G''/G' approaches the constant value $\tan(\Delta\pi/2)$, both below and above T_g. At low frequency ($\omega \rightarrow 0$), it increases linearly below T_g and decreases linearly above T_g.

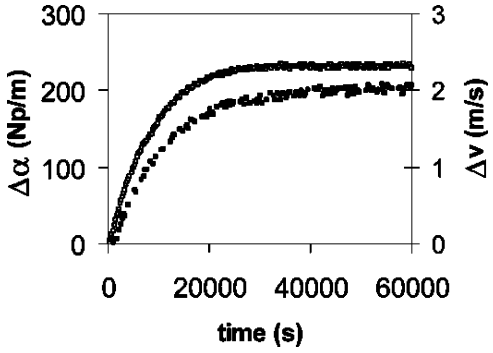

Figure 4. Variation with time of the relative attenuation $\Delta\alpha$ (□) and the relative velocity Δv (■), at 25 MHz during the gelation of Pe 1 30 120.

the absorption increases sharply and then approaches a steady state. The variation of the velocity is very slight (~2 m/s), but the curve has the same general shape as the absorption data. With the estimated accuracy of the method being 0.5 m/s, we ignored the very slow increase over the first four points. The steady change in absorption and velocity is clearly the result of the network formation, but the smooth evolution does not provide a method for a direct distinction of the different stages of the aggregation process.

We now attempt a scaling analysis of the ultrasonic data, as suggested in eq 4. As the gel point cannot be determined directly from the ultrasonic data but has been measured accurately from rheology, we use the rheological value for T_g.

In Figure 5, $(\Delta\alpha v^3)^{-1/k_\infty}$ and $(\Delta v^2)^{1/t_\infty}$ are plotted as a function of time. For both data sets, T_g is fixed at $T_g = 3058$ s, which determines the exponents $k_\infty = 1.20(1)$ and $t_\infty = 0.88(5)$. The value of the exponent k_∞ is highly sensitive to the fit, whereas t_∞ hardly varies. Figure 5 shows that the data points fall well on a straight line, which confirms the scaling proposed by eq 4. Furthermore, the fit for t_∞ holds over a remarkably large time range. As suggested in ref 15, the high-frequency exponents obtained from fitting the ultrasound data differ significantly from the rheological low-frequency exponents. The values obtained here also differ from those measured by Sidebottom for epoxy resins, $k_\infty = 4$ and $t_\infty = 0.47$.[15] This might be related to the fact that the physical gels investigated here contain much solvent, in marked contrast with epoxy resins.

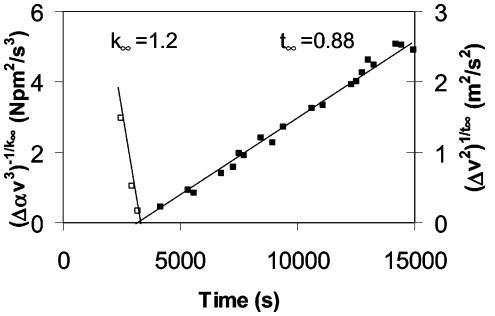

Figure 5. Scaling analysis of the ultrasonic data for Pe 1 30 120. $(\Delta\alpha v^3)^{-1/k_\infty}$ (□) and $(\Delta v^2)^{1/t_\infty}$ (■) are plotted against time. The exponents $k_\infty = 1.2(1)$ and $t_\infty = 0.88(5)$ such that the linear data fits cross the time axis at the rheological gel point $T_g = 3058$ s.

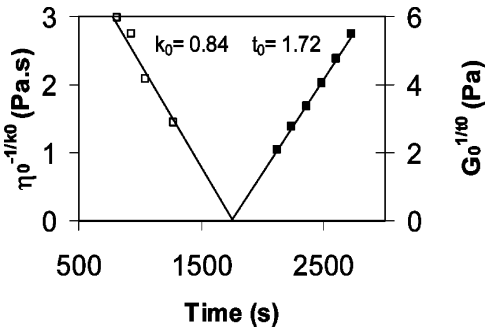

Figure 6. Scaling analysis for the rheological data of the Pe 1 15 30 sample. The best straight line fits for η_0^{-1/k_0} (□) and G_0^{1/t_0} (■) are obtained for $k_0 = 0.84(1)$ and $t_0 = 1.72(1)$, respectively, with the common value $T_g = 1759$ s for the gel time.

3.1.2. Gelling by $CaCO_3$. As an alternative way to introduce calcium ions, $CaCO_3$ has been used. In this case, gelation takes place at a pH close to 7 (final pH ≈ 6).

In Figure 6, the scaling analysis of Figure 2 is applied to the rheological data of the gelation of a 1% (w/w) pectin solution with 15 mM of $CaCO_3$ and 30 mM of GDL (Pe 1 15 30). The gel point, as determined by the modulus G_0 and the viscosity η_0, is at 1759(20) s, and the exponents are estimated at $k_0 = 0.84$ and $t_0 = 1.72$, again in good agreement with theory. A more refined analysis of the frequency dependence of G' and G'' shows scaling over a much smaller frequency range than for Pe 1 30 120.

In Figure 7, we plot the ratio G''/G' against frequency for measurements for increasing times (from top to bottom). The expected increase of G''/G' with decreasing ω below the transition is only observed in the upper frequency range because of the limited sensitivity of the rheometer at low frequency. Only beyond 1650 s is the signal strong enough to have reliable data for all frequencies. Then, the plateau at high frequency and the changing slope at T_g at low frequency become visible. The expected scaling and the value $G''/G' = \tan(\Delta\pi/2) = 2.04$ of the plateau level can be identified only for frequencies below ~3 Hz. A possible explanation for the reduced scaling range in ω of the CaEGTA system is that the system is inhomogeneous due to the localized release of the Ca into the solution. In fact, the $CaCO_3$ powder may not be completely dissolved, thus creating inhomogeneities in the Ca concentration which leads to small aggregates and to an inhomogeneous gel. This will influence primarily the short scale, high ω measurements.

As for Pe 1 30 120, we have applied the Winter−Chambon analysis to the CaEGTA system, expecting fewer fluctuations than in the former case. Indeed, the curves for different frequencies are very stable, and they all cross at $T = 2095(50)$ s with $\Delta = 0.57(3)$. These values differ considerably from the ones from the other analyses. The more detailed analysis of Figure 7 explains the discrepancy. The curve for 2120 s appears to be almost perfectly flat with a value of $G''/G' = 1.2$ over the frequency range considered—guaranteeing a unique crossing point in the Winter−Chambon plot. The discrepancy between the two methods can be resolved by noting that scaling is valid in the zero frequency limit and that the curve for 1899 s, which seems below the transition in the Winter−Chambon analysis, actually turns down at low frequency and therefore is past the transition. We conclude that the true transition is around 1750-(100) s and that the measured crossing in Figure 8 is a finite frequency effect.

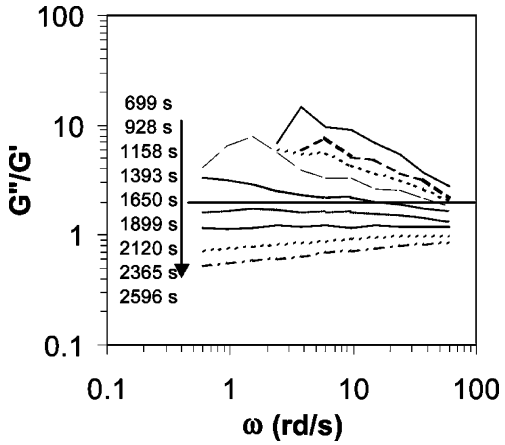

Figure 7. Ratio G''/G' as a function of ω for Pe 1 15 30 (log−log). From top to bottom, the curves correspond to measurements for increasing times. The horizontal line corresponds to the theoretical plateau, $G''/G' = \tan(\Delta\pi/2)$ with $\Delta = 0.71$. At frequencies below ca. 3 Hz, the expected universal scaling can be seen; a change in slope occurs between the data sets for $T = 1650$ s and $T = 1899$s. This fits well with the value $T_g = 1759$ s from Figure 6.

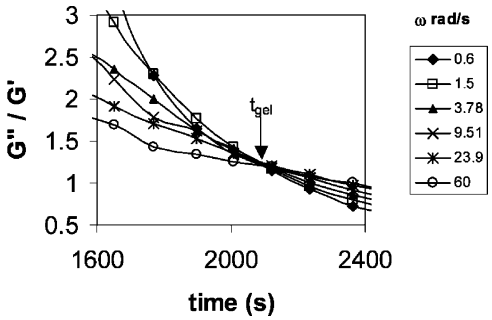

Figure 8. G''/G' as a function of time, for Pe 1 15 30. The different curves are parametrized by frequency ω. The common crossing yields an estimate for the gel point and the exponent Δ.

Ultrasonic measurements were also performed for Pe 1 15 30, and the same scaling analysis as for Pe 1 30 120 was performed. In Figure 9, the exponents k_∞ and t_∞ are adjusted such that $(\Delta\alpha v^3)^{-1/k_\infty}$ and $(\Delta v^2)^{1/t_\infty}$ cross the time axis at the rheological gel time $T_g = 1759$ s. The exponent values $k_\infty = 1.20(2)$ and $t_\infty = 0.89(2)$ and the straight line behavior near T_g again confirm scaling. Both exponents coincide with the ones determined for the Pe 1 30 120−CaEGTA system.

3.2. Alginate Gelation. The gelation of alginate was studied under the same conditions as pectin (1% (w/w) alginate, 15 mM $CaCO_3$, 30 mM GDL). The alginate system gels earlier than the pectin system, because it has a higher reactivity with calcium than pectin.

In Figure 10, the ratio G''/G' versus ω from rheology has been plotted in order to test the validity of scaling. From the

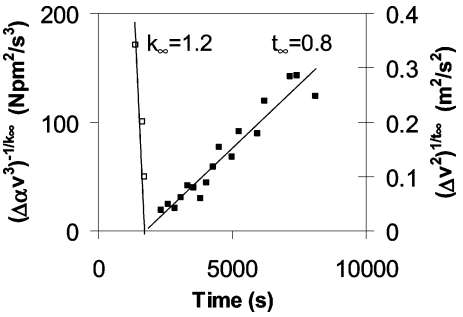

Figure 9. Scaling analysis of the ultrasonic data for Pe 1 15 30. A straight line fit of $(\Delta\alpha\nu^3)^{-1/k_\infty}$ (□) and $(\Delta\nu^2)^{1/t_\infty}$ (■) through the rheological gel point $T_g = 1759$ s determines $k_\infty = 1.20(2)$ and $t_\infty = 0.89(2)$, respectively.

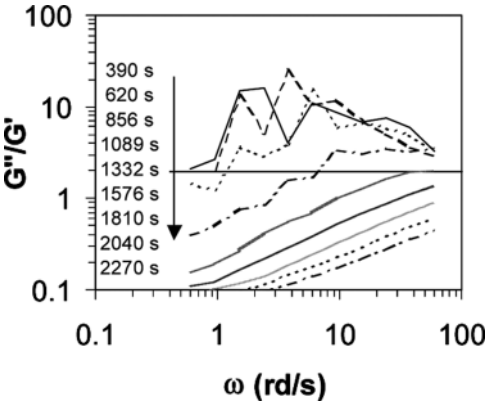

Figure 10. Ratio G''/G' as a function of ω for Al 1 15 30 (log−log). From top to bottom, the curves correspond to measurements for increasing times. Scaling fails altogether. No constant $G''/G' = \tan(\Delta\pi/2)$ scaling regime for large ω and no transition regime with a change of slope for low ω are visible.

figure, it is clear that the expected scaling properties hold nowhere in the accessible frequency range. In particular, there is no high-frequency scaling regime with constant ratio $G''/G' = \tan(\Delta\pi/2)$, and there is no low-frequency range where a change of slope would signal a transition. A possible reason is the inhomogeneities, as already observed for Pe 1 15 30, and which are likely to be more pronounced for alginate because of the higher reactivity. In addition, also because of the faster gelation rate, the system may evolve significantly during the measurements. It is also clear from Figure 10 that a Winter−Chambon-type plot cannot be used, as there is no flat portion anywhere for any of the curves—a necessary condition for a common crossing point.

As the gel point cannot be determined from rheology, another method was used to determine the transition. We noticed that the ultrasonic data has the same general form for all pectin and alginate samples. For both pectin samples, a phenomenological scaling fit of the ultrasonic data near the (rheological) gel point is possible and can be characterized by the same exponents k_∞ and t_∞. Assuming that these exponents are also valid for the alginate sample, the ultrasonic data of Al 1 15 30 can been used to determine the gel point. Such an analysis is presented in Figure 11. The straight line fits for $(\Delta\alpha\nu^3)^{-1/k_\infty}$ and $(\Delta\nu^2)^{1/t_\infty}$ determine two independent estimates of the gel times $T_g = 731(10)$ s and $T_g = 681(35)$ s, respectively. The values of the exponents k_∞ and t_∞ are confirmed by the fact that the straight lines do fit the data.

3.3 Alginate−Pectin Mixture. Our study of alginate and pectin was completed by measurements on several mixtures of the two biopolymers, known to form highly inhomogeneous

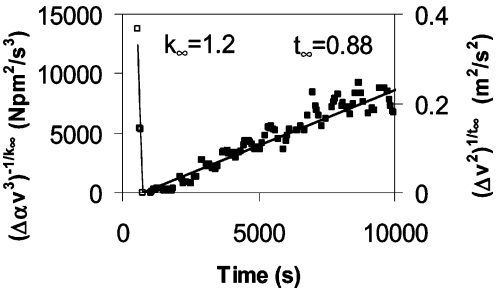

Figure 11. Scaling analysis of the ultrasonic data for Al 1 15 30. $(\Delta\alpha\nu^3)^{-1/k_\infty}$ (□) and $(\Delta\nu^2)^{1/t_\infty}$ (■) are plotted with $k_\infty = 1.2$ and $t_\infty = 0.88$ from the pectin samples. The gel times are $T_g = 731(10)$ s from $(\Delta\alpha\nu^3)^{-1/k_\infty}$ and $T_g = 681(35)$ s from $(\Delta\nu^2)^{1/t_\infty}$.

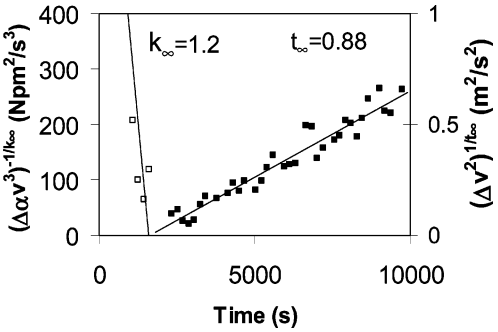

Figure 12. Scaling analysis of the ultrasonic data for the mixing ratio 25/75. $(\Delta\alpha\nu^3)^{-1/k_\infty}$ (□) and $(\Delta\nu^2)^{1/t_\infty}$ (■) are plotted with the values $k_\infty = 1.2$ and $t_\infty = 0.88$, yielding the gel time $T_g = 1669(44)$ s.

gels.[21] Three different alginate/pectin ratios were investigated, with gelation always induced with 15 mM CaCO3 and 30 mM GDL. The total polymer concentration was kept constant at 1% (w/w) in all the samples. The mechanical spectra recorded for these systems are radically different from the ones for the pure systems. Early during the gelation process, $G'(\omega)$ and $G''(\omega)$ cross each other twice in the measured frequency range, excluding any scaling analysis. To understand these systems, one has to keep in mind that the reactivity of alginate with calcium is much higher than the reactivity of pectin with calcium. Therefore, over a wide range of alginate/pectin mixing ratios, gelation is only governed by the calcium/alginate ratio. A decrease in the alginate/pectin ratio therefore leads to an effective increase in the calcium/alginate ratio. For very low alginate concentrations, this even leads to the formation of aggregates, and the system no longer gels macroscopically. A pectin gel with embedded alginate aggregates may still form. These inhomogeneities have been visualized directly by confocal scanning laser microscopy (CSLM).[26] Because of the strong inhomogeneities, rheology at the available frequencies is unable to detect any sol−gel transition.

As ultrasound probes the system very differently from rheology, we attempted to identify the transition in this manner. We have performed attenuation and velocity measurements for alginate/pectin mixtures with ratios 75/25, 50/50, and 25/75. The data were then analyzed like the pure alginate system, assuming the same values for the exponents, $k_\infty = 1.2$ and $t_\infty = 0.88$. The $(\Delta\alpha\nu^3)$ and $(\Delta\nu^2)$ data plotted in scaling form are shown in Figure 12 for the 25/75 mixture. The crossing of the time axis of the straight line fits determines the gel points, $T_g = 1156(44)$ s for the 75/25 mixture, $T_g = 1432(31)$ s for the 50/50 mixture, and $T_g = 1669(44)$ for the 25/75 mixture. The data clearly show that the gel point for the mixtures smoothly interpolates between the gel points of the pure systems. Starting from pure alginate, the gel points rise linearly with increasing

pectin fraction and saturates for high pectin fractions. In other words, adding small amounts of pectin linearly increases the gel time from its alginate value, whereas small quantities of alginate barely lower the pectin gel time.

These results show that ultrasound can be used as a qualitative method to detect the sol−gel transition in cases where rheology is not able to identify the gel point because of inhomogeneities. Our results on alginate and on the mixtures suggest that ultrasound is less sensitive to inhomogeneities than rheology.

4. Conclusions

The first part of the present investigation shows for two pectin samples with a different calcium release mechanism that rheological measurements close to the transition are universally described by scalar percolation theory. For the CaEGTA system, believed to be more homogeneous, the expected scaling form and scaling exponents are recovered over the entire frequency range. For the $CaCO_3$ systems, the theoretical results are only reproduced at low frequency. The difference between the two samples can be explained by inhomogeneities in the gel because of the difference in the calcium release mechanism. There is evidence for the presence of small aggregates around the $CaCO_3$ particles, due to a local increase in calcium concentration.[26]

A comparison of the different methods to identify the transition and measure the scaling properties shows that for a reliable determination of the sol−gel transition properties one must verify the consistency of all the $G(\omega)$ data. For the Pe 1 15 30 case, different results are obtained with the Winter−Chambon method than from a detailed analysis of the frequency dependence of the data. The former predicts—on the basis of measurements at intermediate frequencies—a transition with a higher gel point and a lower exponent Δ than the direct analysis of $G(\omega)$.

The ultrasonic measurements, which probe the gel in a different way, reveal a increase of both the attenuation and the velocity for the two pectin systems studied. A high-frequency scaling analysis determines the ultrasonic critical exponents at the rheological gel point, with values that are the same for both samples but different from the rheological ones.

For the alginate samples, the rheological data cannot be interpreted in terms of scaling theory, and for the alginate/pectin mixtures, there is not even a monotonic behavior of the moduli. The ultrasonic data of alginate and the mixtures, on the other hand, closely resemble the pectin data. Applying the scaling approach that works for pectin to the ultrasonic data of alginate and the mixtures provides an alternative, phenomenological method to determine the gel point. For the mixtures, the gel time determined in this way interpolates between the gel times of the pure systems. The questions regarding whether the ultrasonic data fundamentally is singular at the gel point and whether the associated exponents k_∞ and t_∞ are universal are open questions at present.

References and Notes

(1) Adam, M.; Lairez, D. Sol−gel transition. In *Physical properties of polymeric gels*; Cohen Addad, J. P., Ed.; John Wiley & Sons Ltd.: Chichester, 1996; pp 87−142.
(2) Prochazka, F.; Nicolai, T.; Durand, D. *Macromolecules* **1996**, *29*, 2260.
(3) Axelos, M. A. V.; Kolb, M. *Physical Review Lett.* **1990**, *64* (12), 1457−1460.
(4) Lu, L.; Liu, X.; Tong, Z. *Biomacromolecules* **2005**, *6*, 2150.
(5) Nicolai T.; Randrianantoandro H.; Prochazka F.; Durand D. *Macromolecules* **1997**, *30*, 5897.
(6) Salome L.; Allain C. *Macromolecules* **1987**, *20*, 2958; **1990**, *23*, 981
(7) Flory, P. J. *J. Am. Chem. Soc.* **1941**, *63*, 3083.
(8) Stockmayer, W. H. *J. Chem. Phys.* **1943**, *11*, 45.
(9) Stauffer D. *Phys. Rep.* **1979**, *54*, 1. Stauffer D.; Aharony A. *Introduction to percolation theory*; Taylor and Francis: New York, 1994.
(10) Efros, A. L.; Shkolovskii, B. I. *Phys. Status Solidi* **1976**, *76*, 475.
(11) Luck, J. M. *J. Phys. A: Math. Gen.* **1985**, *18*, 2061.
(12) Winter, H. H.; Mours, M. *Adv. Polym. Sci.* **1997**, *134*, 165.
(13) Chambon, F.; Winter, H. H. *Polym. Bull.* **1985**, *13*, 499; *J. Rheol.* **1987**, *31*, 683.
(14) Povey, M. J. W. *Ultrasonic Techniques for Fluids Characterization*: Academic Press: San Diego, 1997.
(15) Sidebottom, D. L. *Phys. Rev. E* **1993**, *48*, 391.
(16) Pindinelli, C.; Montagna, G.; Luprano, V. A. M.; Maffezzoli, A. *Macromol. Symp.* **2002**, *180*, 73.
(17) Audebrand, M.; Doublier, J. L.; Durand, D.; Emery, J. R. *Food Hydrocolloids* **1995**, *9*, 195.
(18) Bacri, J. C.; Courdille, J. M.; Dumas, J.; Rajaonarison, R. *J. Phys., Lett.* **1980**, *41*, L369.
(19) Ratajska-Gadomska, B.; Gadomski, W. *J. Phys.: Condens. Matter* **2004**, *16*, 9191.
(20) Lairez, D.; Durand, D.; Emery, J. R. *Makromol. Chem., Macromol. Symp.* **1991**, *45*, 31.
(21) Smidsrod, O. *Faraday Discuss. Chem. Soc.* **1974**, *57*, 263.
(22) Axelos, M. A. V.; Mestdagh, M. M.; François, J. *Macromolecules* **1994**, *27*, 6594.
(23) Draget, K. I.; Skjåk-Bræk, G.; Stokke, B. T.; *Food Hydrocolloids* **2006**, *20*, 170 (24).
(24) Axelos, M. A. V. *Makromol. Chem., Macromol. Symp.* **1990**, *39*, 323.
(25) Stokke, B. T.; Draget, K. I.; Smidsrod, O.; Yuguchi, Y.; Urakawa, H.; Kajirawa, K. *Macromolecules* **2000**, *33*, 1853.
(26) Audebrand, M.; Garnier, C.; Kolb, M.; Axelos, M. A. V. Gelation of pectin-alginate mixtures: Ultrastructure and rheological properties. Proceedings of *Int. Symp. Food Rheol. Struct.*, Zürich, February 9−13, 2003, ETH Zürich.

BM060297E